

A PARAMETRIC STUDY OF THE BEHAVIOR OF GEOSYNTHETIC REINFORCED SOIL SLOPES

R. Qhaderi

Former postgraduate student of Geotechnical Engineering, IUT, Iran

M. Vafaeian and H. Hashemolhoseini

*Lecturer, Isfahan University of Technology, Isfahan, Iran,
mahmood@cc.iut.ac.ir, hamidh@cc.iut.ac.ir*

(Received: Nov. 2, 2004)

Abstract This paper presents the results of a number of computations using the 2D FEM to show the effects of significant variables on the behavior of geosynthetically reinforced earth slopes. The verification and reliability of the results are primarily examined through comparisons with experimental data available. The results seem to be quite acceptable and can be used with a high degree of reliability for predicting the relevant problems.

The main variables studied are soil properties, slope geometry, and the properties of reinforcement elements, while the safety factor, deformation components, effect of geotextile stiffness, the shape and location of the slip surface are the main unknowns sought.

Keywords Reinforced earth slope, Geosynthetic, Effective parameters, Safety factor

چکیده در این مقاله، نتایج حاصل از محاسبات انجام شده به وسیله نرم افزار اجزای محدود در خصوص بررسی رفتار شیبهای خاکی مسلح به ژئوسنتتیک ارائه می شود. با توجه به اینکه هدف اصلی این محاسبات، بررسی و تحلیل تأثیر عوامل مؤثر بر پایداری و دگرشکل‌های شیبهای خاکی مسلح است، از این رو متغیرهای انتخاب شده در این تحلیلها عبارت است از: خواص مهندسی خاک مثل چسبندگی و ضریب اصطکاک، مشخصه‌های هندسی خاکریز مثل شیب و ارتفاع، سختی ژئوتکستایل و تعداد و زاویه آنها.

نتایج حاصل از این محاسبات را می توان با اطمینان کافی در ارزیابی رفتار شیبهای مسلح مورد استفاده قرار داد و این اطمینان به این علت است که نه تنها صحت نتایج و منطقی بودن روش محاسبات به وسیله مقایسه نتایج با بعضی از اطلاعات تجربی در دسترس کنترل و تأیید می گردد بلکه مجموعه نتایج محاسبات به نحو قابل قبول و سازگار با یکدیگر همخوانی و همبستگی منطقی نشان می دهد.

1. INTRODUCTION

Reinforced soil slope has been the subject of extensive research in the geotechnical field within the past 25 years, resulting in numerous publications on experimental results and theoretical analyses. Since H. Vidal (1969) proposed the mechanism and application of

reinforced earth, many aspects of this topic have been investigated. Moreover, at least seven international conferences have been so far held on the subject of the Geosynthetics.

Nevertheless, as application of new techniques or development of new finite element software promise attractive results and innovative applications, the field is still open to study from

both theoretical (better understanding) and practical (design procedure) viewpoints.

Generally speaking, studies of geosynthetically-reinforced soils can be categorized into analytical, experimental, or numerical types. According to Michalowski (1990), analytical studies of reinforced soil slopes can further be subdivided into three main groups. The first group is based on the conventional slice method, examples including studies by Reugger (1986) and Wright and Duncan (1991). The second, often called "structural method", engages limit equilibrium analysis or the rotational equilibrium analysis. Among the studies based on this method, one can mention Schmertmann et al. (1987), Leshchinsky and Boedecker (1989), Jewell (1991, 96), and Michalowski (1990). The third group of analytical studies involves some kind of homogenization techniques such as those often employed in the analysis of composite materials, where the non-homogenous reinforced soil (soil and geotextile) is modeled as an anisotropic homogenous material. This method is also called "continuum method". The approach by Sawicki and Lesniewska (1989) belongs to this group of studies.

During the last decade, outstanding experimental studies have been carried out on reinforced soil slopes. These studies, which are sometimes supplemented by numerical and analytical analyses, are performed either on real models (field dimensions) such as Chalaturnyk et al. (1990), or on reduced models by centrifugal apparatus such as Porbaha and Kobayashi (1998) and Zornberg et al (1998).

Nowadays, the numerical methods, and mainly finite element, have won universal acceptance in the geotechnical domain. Using appropriate constitutive models for soil and soil-structure interfaces and effective numerical techniques such as the arc length makes it possible to obtain a realistic model of reinforced soil slopes.

A review of about 13 previous experimental studies (from 1990 to 1998) have been reviewed by Zornberg and Arriaga (2000) in which the heights of slopes varied between 2.7m to 7.6 meters (with only one case of a slope with a height of 27.4 m).

Despite the rather numerous studies conducted on reinforced soil slopes, a number of important points still remain to be resolved. One such point

in need of clarification is the effects of geotextile stiffness and soil dilation on the stability of reinforced soil slopes and on the shape of shear band (failure surface). Using 2D finite element method, the present study aims to shed light on this issue. Here, a generic algorithm is used as a post-treatment tool to FEM for fitting an appropriate curve (circle or spiral) to failure surface.

2. BASIC VARIABLES FOR THE COMPUTATIONS

The Plaxis 2D program has been used to investigate a parametric study of reinforced cohesionless soil types. The type of reinforcement layers assumed in this study simulates the geosynthetic sheets embedded within the soil layers while overturning on the top of each layer at the front edge of the slope (as the facing). The soil properties and the reinforcement design arrangements for the purposes of the present study have been chosen within the following ranges:

Soil: $\phi = 28$ to 43 degrees; $\psi = 0$ to 10 degrees; $c = 10$ kPa; $\gamma = 20$ kN/m³

Slope geometry:

Slope angle:

$\theta = 45^{\text{D}}$ to 73^{D} , *Height = 6m to 18m*

Reinforcement design parameters:

EA (tensile stiffness): 150 to 10000 kN/m

Number of Layers: 10 to 30

Length of reinforcement sheets: 2 to 12 m

Angle of reinforcement relative to the horizontal axis: 0 to 20^D

The two dimensional mesh is generated by the automatic option composed of triangular elements including 15 nodes.

The output results computed by the program can be classified as follows:

1. Distribution of tensile stresses along each layer (kN/m);
2. Distribution of maximum tensile stress along the height of embankment;
3. Distribution of tensile strain on the vertical cross section;
4. Maximum amount and distribution of horizontal, vertical, and total displacements along the height;

5. Deformed mesh corresponding to the final stage of computation;
6. Shape and location of critical surface; and
7. Safety factor for each computation.

Both models of work-hardening and elastic Mohr-Coulomb were applied for the computations and the results were compared for any differences. Finally and based on the comparisons, the work hardening approach was selected. The selection is primarily based on the fact that the constitutive model which used in these analyses could not always reach a consistency and convergence. There are two technical points that should be mentioned for this matter:

1) In many elastic – plastic problem regarding the soil medium – rather than the slope stability-application of elastic –Mohr Coulomb in a finite element program does not face to an un convergency, while the computation procedure in slope stability may sometimes reach to a point of collapse at which the computation can not proceed further.

2) The concept of safety factor in slope stability is commonly based on the ratio of resisting agents to the disturbing agents (either in terms of forces or the moments) along a predefined trial and assumed failure surface. On the other hand, within the F. E. M. programs for the soil medium the procedure of c- ϕ reduction is applied and the safety factor defined as the ratio of the actual existing values of these parameters to the reduced values which correspond to the collapse. The results of these two computations may be different specially for the reinforced soils but not for a simple soil medium.

3.RESULTS

It is universally known that both geometric and physico-mechanical properties of reinforced slopes are effective factors in slope behavior and stability. We first begin by comparing the FEM results with other analytical or experimental data; below are selected examples:

1) A comparison is made between the results obtained from Plaxis and those from the methods proposed by Janbu and Bishop (GEOSLOPE

downloaded from the Internet) for the safety factor values on a non-reinforced slope of 7.2m high with $\theta = 27^{\circ}$ to 63° , $c = 10kPa$, $\gamma = 20kN/m^3$ and the friction angle of 37° . This comparison is shown graphically in Figure 1 A similar comparison is presented in Figure 2 for the variations of friction angle from 20° to 45° for the same conditions and the slope angle of 45° .

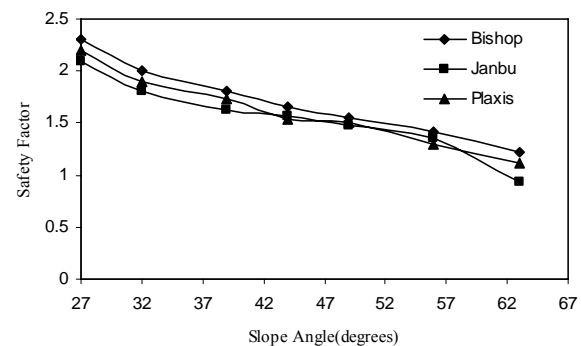


Figure 1. Comparison of computed safety factor in three methods for the slopes with different slope angles.

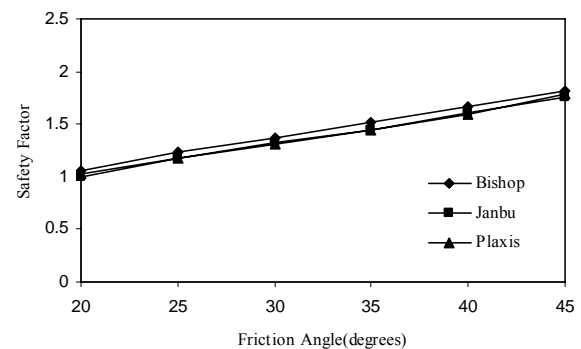


Figure 2. Comparison of increasing the safety factor in three methods of computations for different values of friction angle.

2) A simple example of actual reinforced slope (Fannin and Hermann,1990), as shown in Figure 3a, with a height of 4.8m, slope of 1H:2V, and reinforced with 8 large reinforcements (0.6m separation) with tensile stiffness of EA=150 kN/m is selected for the case study. The soil properties are as follows:

Friction angle $\phi_{pl.st.} = 38^\circ$ and $\gamma = 17 \text{ kN/m}^3$.

The measured values of tensile forces in the reinforcement elements obtained from comparisons for the forces is illustrated in Figure 3b.

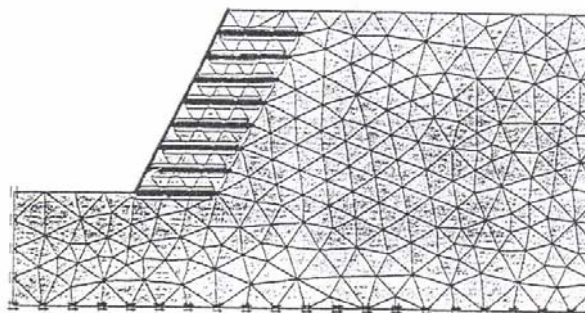
In Figure 3c, a comparison is made between the results obtained from Plaxis and the measured values for the vertical stress at levels 0.3, 1.5, and 2.7m from the base at a section of 1.5m from the slope face.

3) Another actual case is analyzed to compare the tensile forces within the reinforcement elements. Figure 4a shows the vertical section of a reinforced

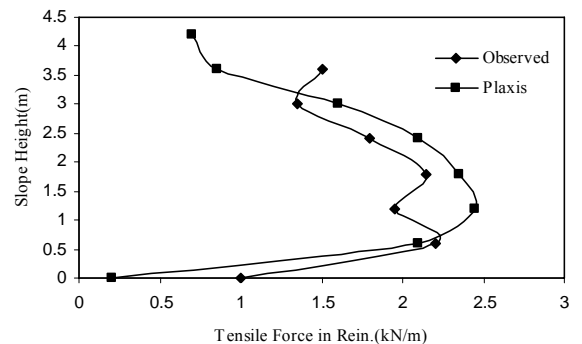
step-wise slope wall in Italy (reported by Ghinelli and Sacchetti, 1998) with soil properties of $\gamma = 18.4, \phi = 33^\circ, c = 0, E_s = 35.2 \text{ MPa}, \nu = 0.2$, $H=15.5\text{m}$, and a reinforcement tensile stiffness of 500 kN/m. Typical comparisons are shown in Figure 4b between the results of the present study by Plaxis and the results of F. E. M. by Ghinelli and Sacchetti (1998) for the tensile forces along the reinforcement layers of C, D, E, L and M as indicated in Figure 4a.

These examples promoted confidence about the correct use of Plaxis.

To evaluate the effect of each variable on the different aspects of slope behavior, several computations were carried out, and the results were categorized graphically in Figures 5 to 11 as described in Table 1.

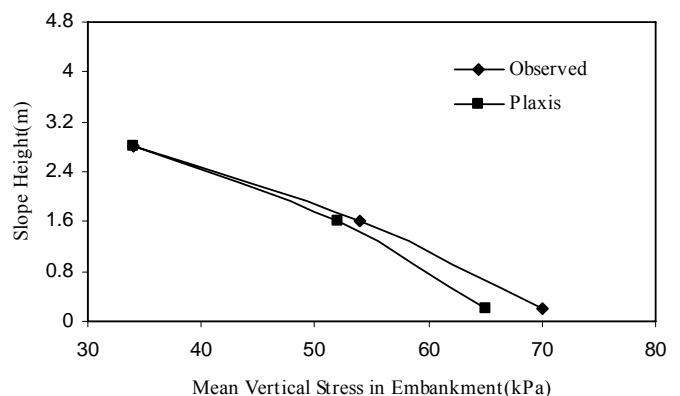


(a)



(b)

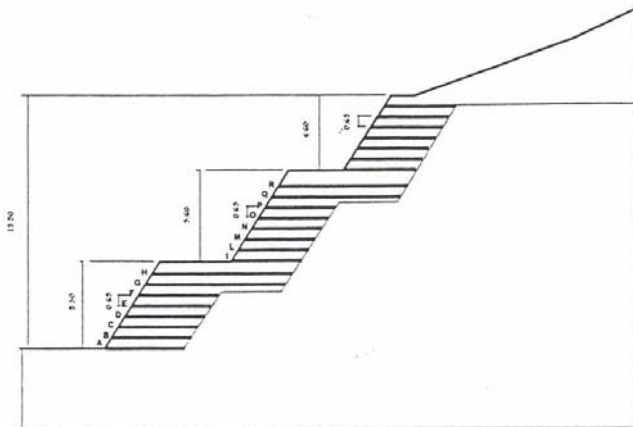
Figure 3. (a) Cross section of an actual case of reinforced slope, (b) Comparison between the computed and measured values of distribution of maximum tensile force in reinforcement layers of Fig. a; (c) Comparison between the computed and measured values of mean vertical stresses along depth.



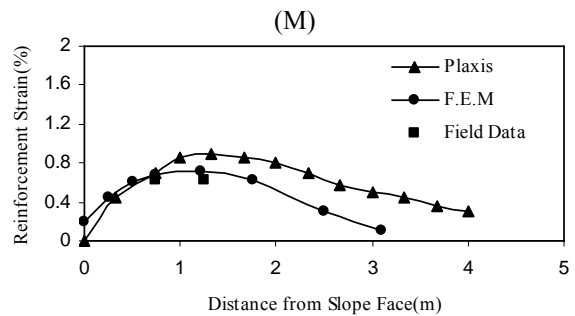
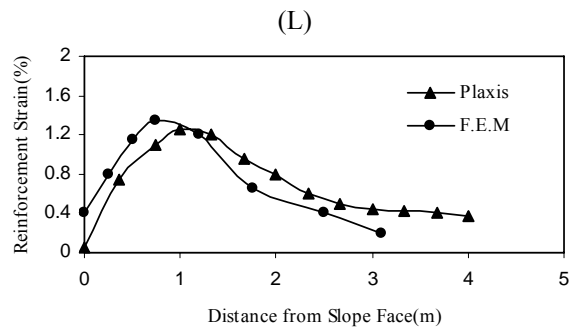
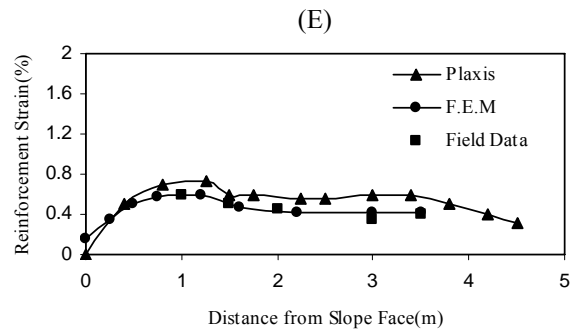
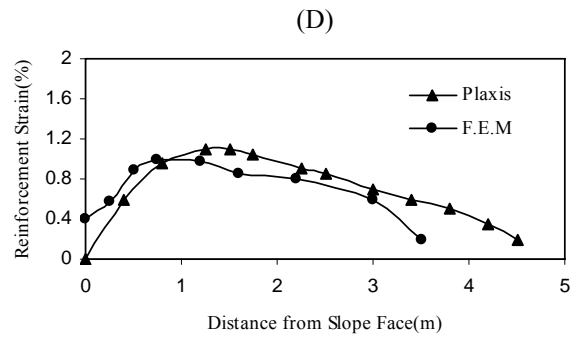
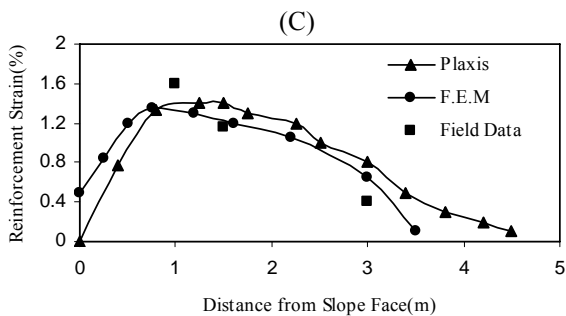
(c)

Table 1. Discription of Figures

Effects	In Figure
EA from 150 to 1000	5
Angle of slope	6
Soil friction	7
Height of slope	8
Number of reinforcements	9
Length of reinforcements	10
Reinforcement slope	11



Geometrical Dimensions of Embankment



F.E.M.: (Ghinelli & Sacchetti, 1998) Plaxis: (present study)

Figure 4 (a): Cross section of an actual stepped reinforced soil slope, (b) Comparison between the computed and measured values of tensile strain along some selected layers (C,D,E,G, L and M) of reinforcement corresponding to the stepped slope.

In these Figures, the variations in tensile stress are shown in part (a) and the variations in safety factor are shown in part (b) while the values for displacements and shear strains are shown in parts (c) and (d), respectively.

An example of deformed mesh after failure and computed shear band is shown in Figures. 12 and 13, respectively.

4.DISCUSSION

The present results can be viewed from (at least) 3 aspects:

- a) The effect of changing the properties of soil and/or reinforcement on the computed values of deformations, internal stresses and the overall calculated safety factor.
- b) The location and the shape of failure surface;
- c) Comparisons and some complements for practical purposes.

a) The effect of variables on the computed values

As expected, the slope angle and the slope height are the first and the main design requirements affecting stability or safety factor (Figures. 6b and 8b) and the deformation field (parts c and d in Figures. 6 and 8). The length of reinforcement elements by up to a length of $0.8H$ to $0.9H$ has some clear effects; but beyond that, higher lengths do not show any significant effect on the internal stability (Figure 10), though it should be checked for the pooling out safety. Increasing the stiffness of reinforcements (Figure 5b) and/or increasing the soil strength result in some higher safety factors (Figure 7b) and fewer deformations (Figures 5c and d, and 7c and d).

This type of response is quite predictable because of the interdependence of deformations and stiffness. Similar results have been reported by Han, Leshchisky and Shao (2002) for a computed case by FLAC in which they used the stiffness values from 200 to 4000 kN/m for cable elements in a slope with $H=5$ m, a slope angle of 45° , composed of a cohesionless soil with $E=20$ MPa and $\phi = 30^\circ$. The effect of increasing stiffness is also clear on the maximum tensile stress along the reinforcement elements (Figure 5.a)

The present computations and graphs indicate that the values of strains corresponding to the least safety factor approximate rather large values, at least 2% (part d in Figures. 5 to 11). From this correlation, one can conclude that the failure of soil corresponds to the residual angle of friction (rather than the peak angle). Also the angle of dilatancy of sand does not show any (even small) effects on the results.

b) Shape of failure surface

As indicated in the literature, the geometrical shape of failure curve can be a matter of discussion in classical analytical computations and also in experimental observations.

The shape of failure surface cross section or the shear band can simulate both, with some approximations, circular and spiral curves in the first qualitative look, as illustrated in Figure 13. Nevertheless, analytical computations show that a circular curve can be better fixed with the view of obtained shear band.

Our computations indicate that the location of the shear band (zone) somehow depends on the overall stiffness of the slope–reinforcement system because when the reinforcement stiffness increases, this zone moves farther from the slope face. This finding can be seen by comparing parts a, b, and c in Figure 13.

In these computations, the shape of failure (shear band), shown by Plaxis, is sometimes quite clear while under some other conditions a wide band (or even a shadowy band) is obtained from which a sharp and deterministic curve can hardly be concluded. However, it is usually promising to pursue the place of plastic points of F.E. mesh (as in Figure 14) from which its limiting boundary can be the representing position of failure curve.

Though the failure/shear band can be clearly traced on the vertical sections, the safety factor against the failure is not linearly dependent on the stiffness values of reinforcement (Figure 5b), on the friction angle of soil (Figure 7b), nor on reinforcement values (Figure 9b)

However, it is concluded from the figures that the amounts of deformation and maximum shear strain can be selected as variables indicating the differentiation between the stable and unstable cases (parts c and d in the Figures).

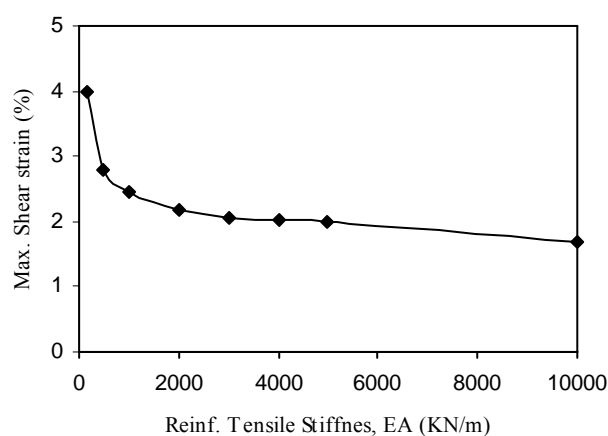
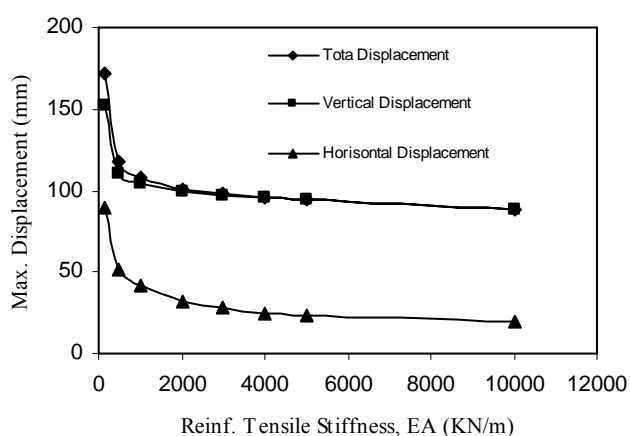
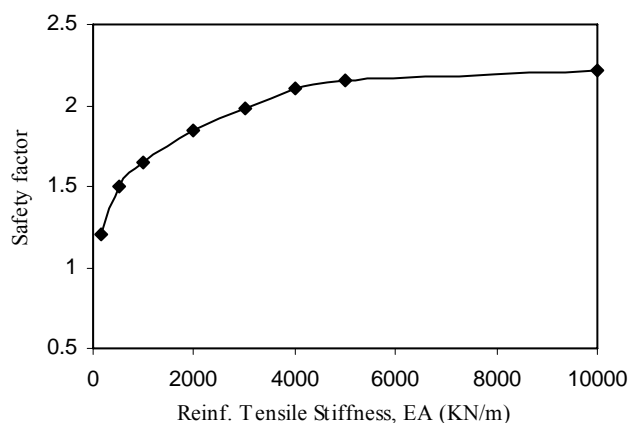
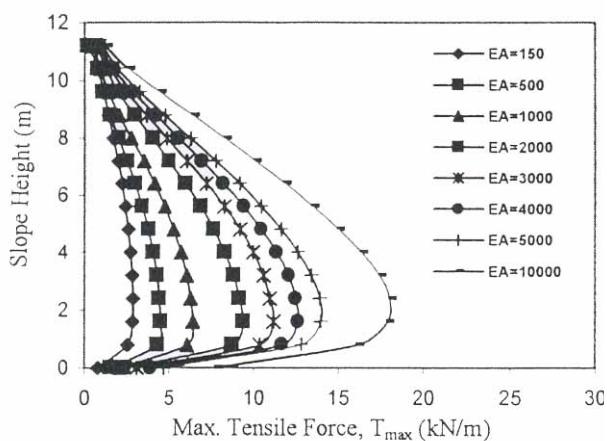


Figure 5. Computed effect of tensile stiffness of reinforcement elements (from 150 to 10000 kPa) on: (a) the values of maximum tensile forces (T_{max} , kN/m) and its distribution along the depth, (b) the factor of safety, (c) displacement and (d) Max, shaar strain

The computed results indicate that the location of failure zone depends to some extent upon the slope angle, length of reinforcements, and on their tensile stiffness. Increasing the slope angle will cause the failure zone to move deeper through the embankment. Also with increased stiffness, the failure bond moves deeper through inside and tends to occur within the non-reinforced part. Considering the above facts, deciding about the real geometrical shape of failure curve (whether circle or spiral) can always be a matter of uncertainty. Nevertheless, a number of mathematical tools presently exist that may be employed to show the comparative advantage of one assumption over another.

For our present purposes and in order to find a best and compatible curve for the failure shape computed by Plaxis, the following prerequisites are primarily mentioned.

Because different variables may affect the behavior of soil-reinforcement system, the failure curve should also be discussed for some different selected cases; hence, this is considered for the computed results with 5 different values of stiffness modulus, 3 different numbers of reinforcement layers, 3 values for slope angle, 3 values for slope height, and 3 values for soil friction angles. In Table 2, the data for these cases are presented.

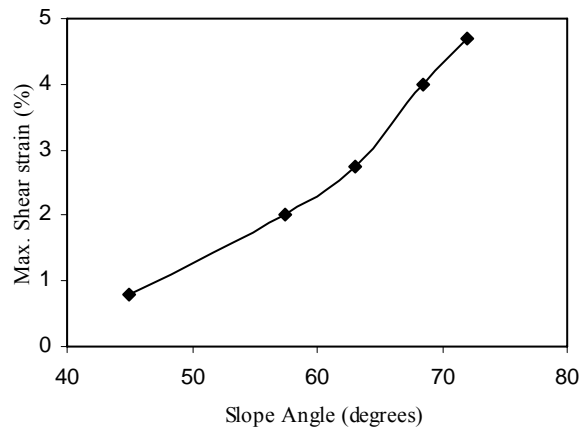
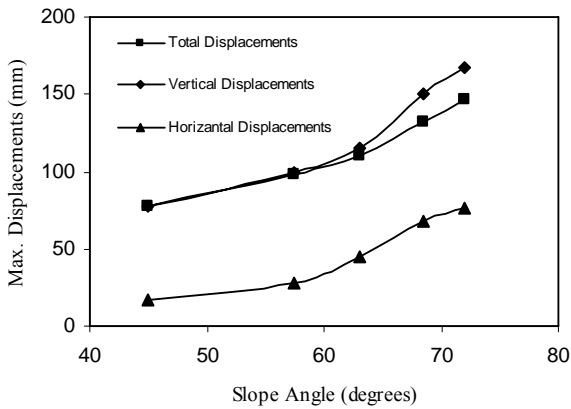
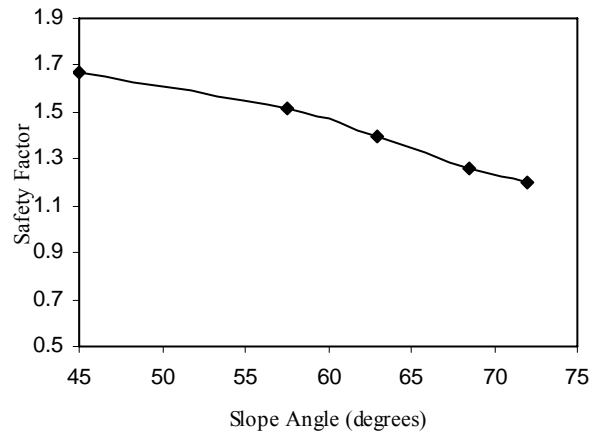
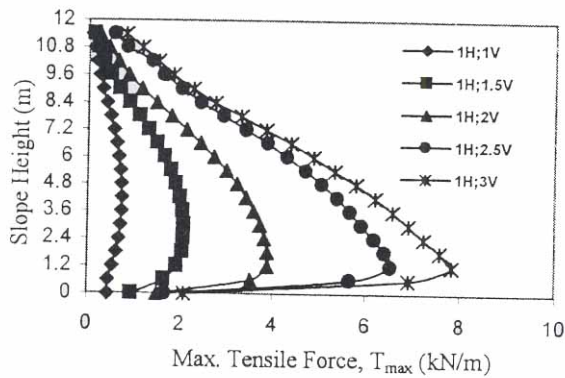


Figure 6. Computed effect of slope angle of wall on the same variables as in figure 5.

To find the best mathematically-fitted curve to the computed failure curve, a computer program of genetic algorithm is used. This program is compiled on the basis of C++ computations and applied as the tool for finding the curve of best fitting based on stochastically non-linear optimization procedure (Michalewicz, 1992). The optimization criterion for the curve is based on the minimizing statement:

$$\sum_{i=1}^n \left\{ R_i^2 - (x_i - x_c)^2 - (y_i - y_c)^2 \right\}$$

where, n is the number of given points on the accepted curve considered, x_i and y_i are the coordinates of the points, and x_c , y_c and R_i are coordinates of the spiral center and its radius, respectively, as shown in Figure 15.

The representing formula for the spiral is $R = a \cdot \exp(-\beta \cdot \tan \varphi)$

where, R is constant for a circular curve.

The best-fitted curve is accepted by minimizing the sum of square of errors (MSE) as:

$$MSE = \frac{1}{n} \sum_{i=1}^n \sqrt{(x_0 - x_i)^2 + (y_0 - y_i)^2}$$

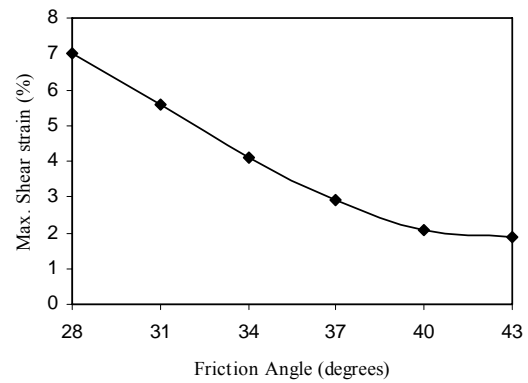
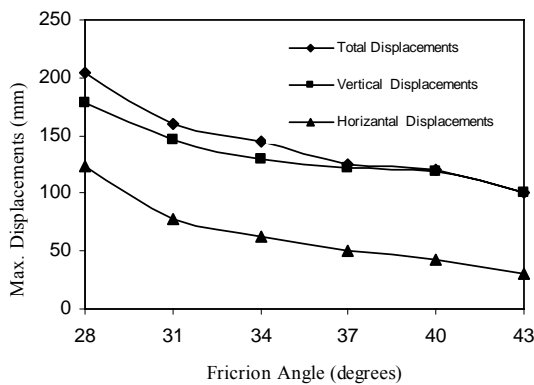
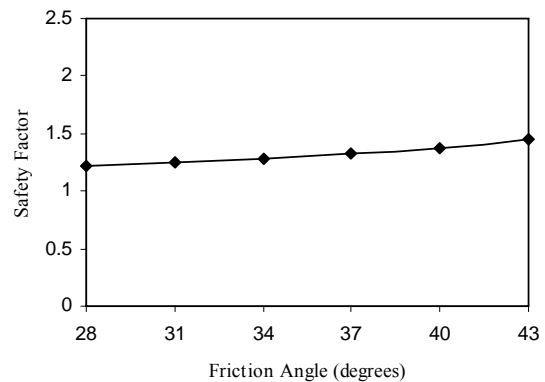
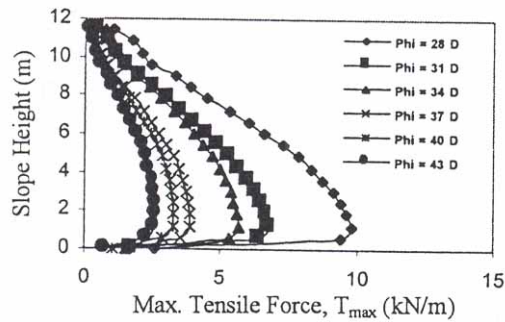


Figure 7. Computed effect of friction angle of soil on the same variables as in figure 5.

where, x_i and y_i are the coordinates of the points corresponding to the sliding curve obtained from the present finite element method and x_0 and y_0 are the coordinates of the points of the fitted curve.

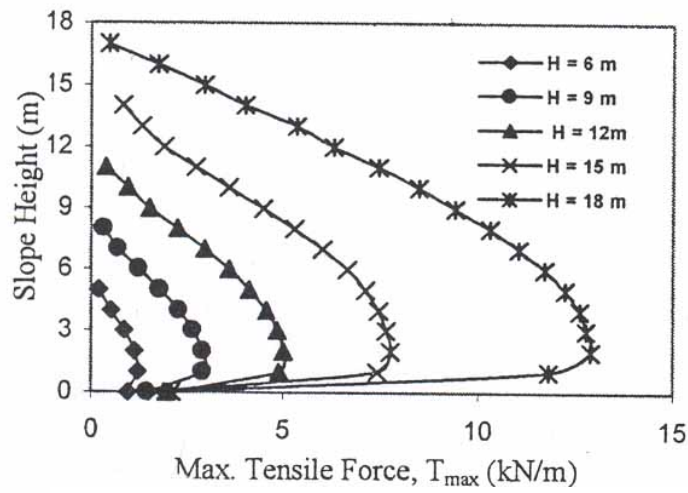
In Table 2, the computed values for MSE are shown for the assumed and computed cases for both spiral and circular curves for the 17 cases considered in the present study. Because these numbers are far smaller for the circular shape than for the spiral one, the circular curve is more acceptable.

Figures 16 and 17 illustrate examples of the

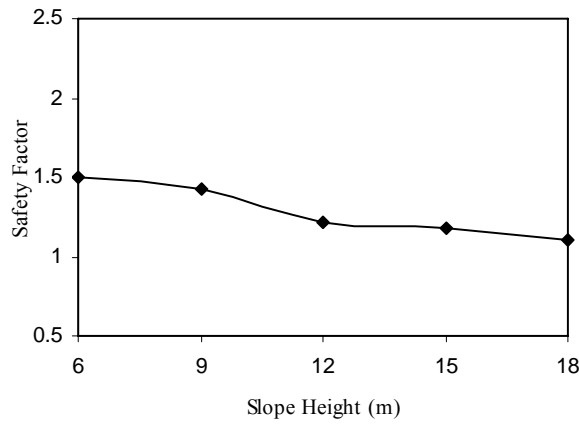
best-accepted curve for the computed failure curve and the best-fitted curves of spiral and circle shapes for which the values of MSE are shown in Table 2. Figure 15 shows two cases with different values of $EA=150$ and 5000 kN/m, and Figure 16 shows two cases with different values for different numbers of reinforcement layers ($N= 10, 30$) but for the same slope.

c) Some practical compliments

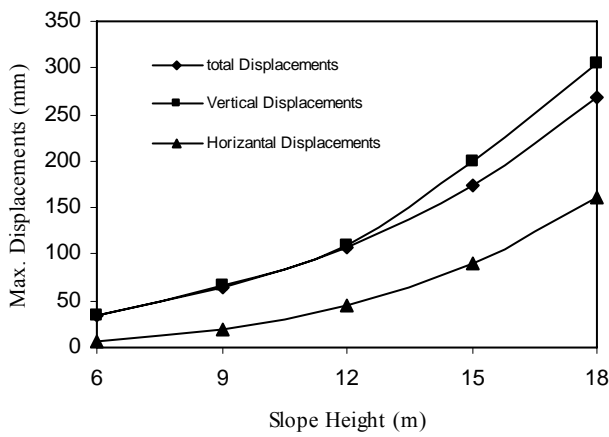
There is no agreement on the shape of maximum tensile stress distribution within the reinforcement layers along the height as shown in Figure 18



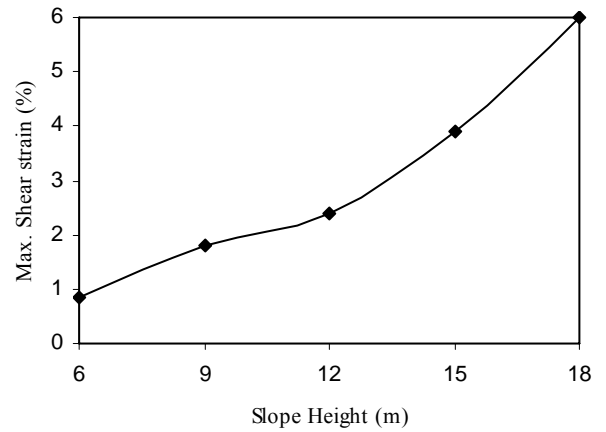
(a)



(b)

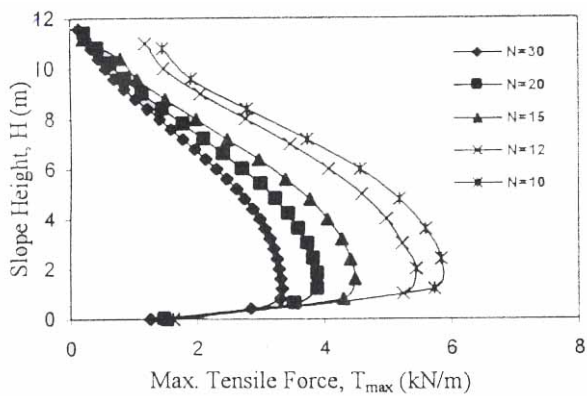


(c)

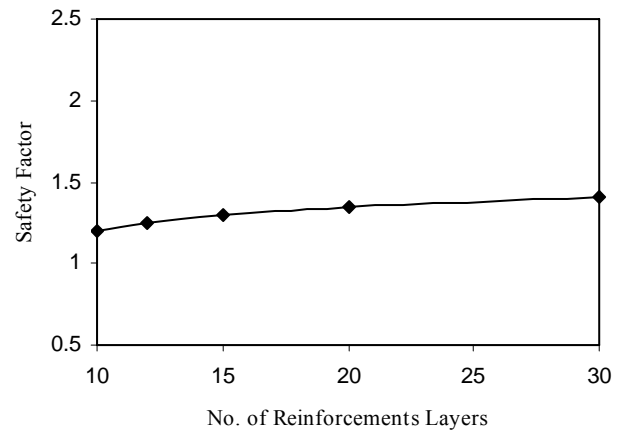


(d)

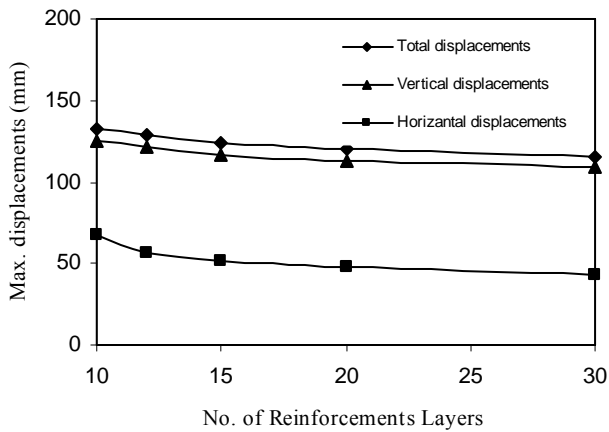
Figure 8. Computed effect of the height of wall on the same variables as in figure 5.



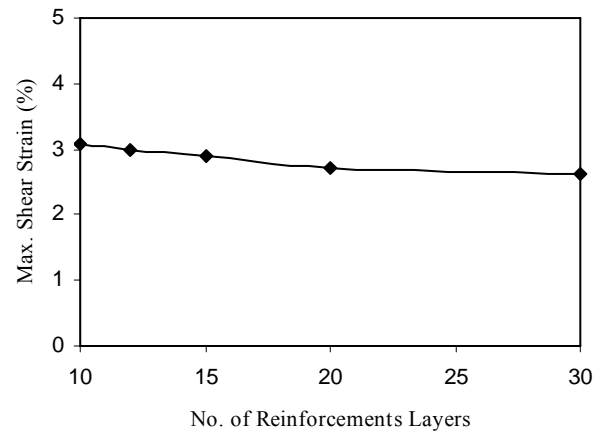
(a)



(b)



(c)



(d)

Figure 9. Computed effect of the number of reinforcement layers on the same variables as in figure 5

(Zornberg et al. 1998). Our computations showed that the best compromise that can be accepted is the one shown in Figure 18, which is almost a linear distribution with the maximum value near the base (see part a in Figures. 5 to 11). This type of distribution of maximum tensile forces along the height is in agreement with experimental data obtained (see Figure 3).

On the basis of the shear strain contour lines and also from the graphical view of the shear band (Figure 13), the location of maximum shear strain may be localized at the intersection of the vertical line passing through the top edge of the slope and the shear band curve (line ab in Figure 15). This means that it should be possible to increase the stability and safety of the slope by strengthening this pointed zone.

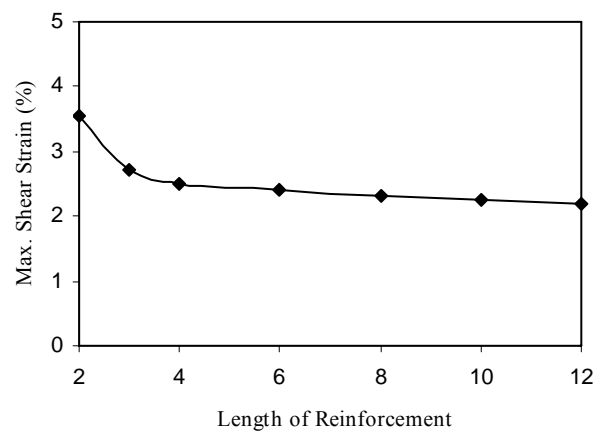
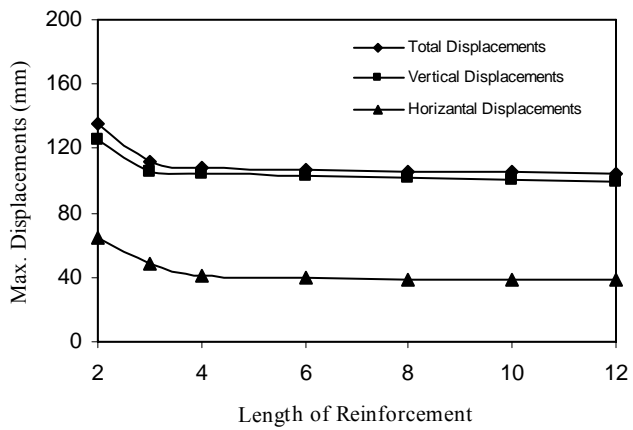
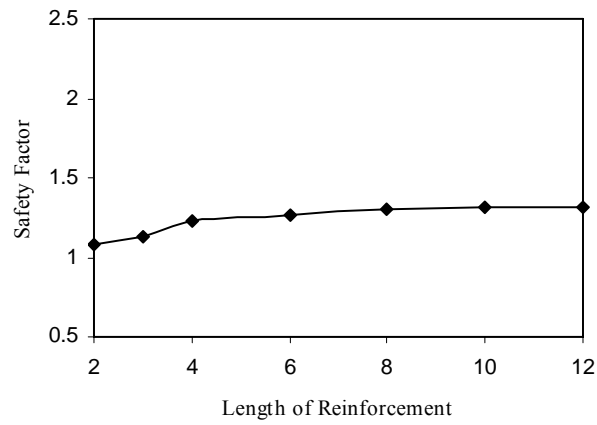
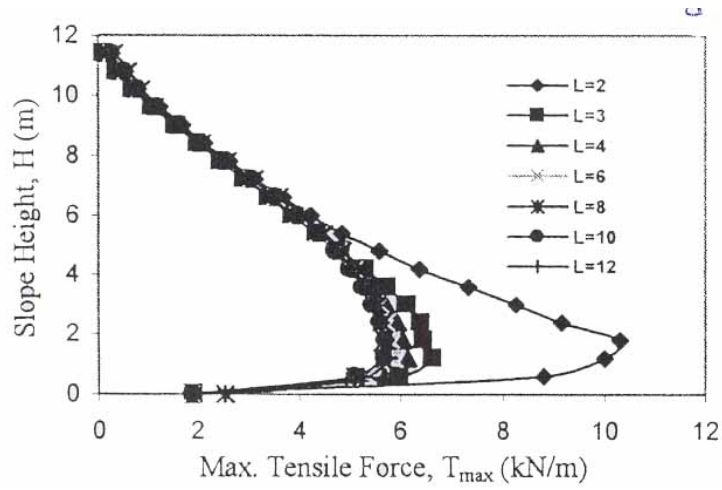
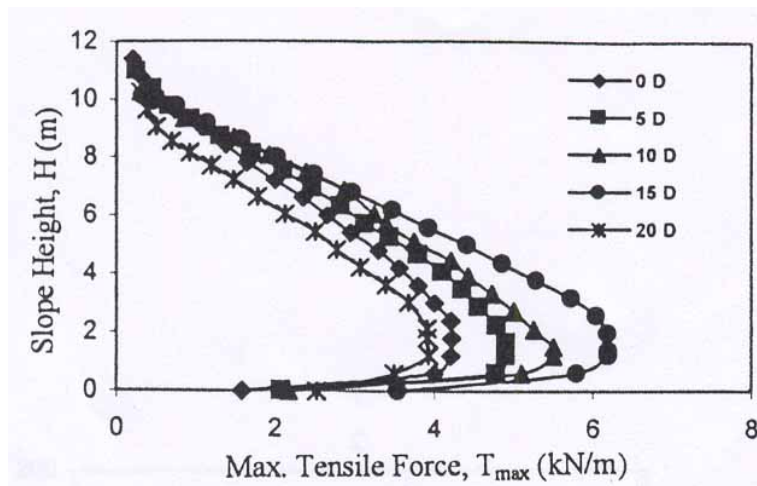
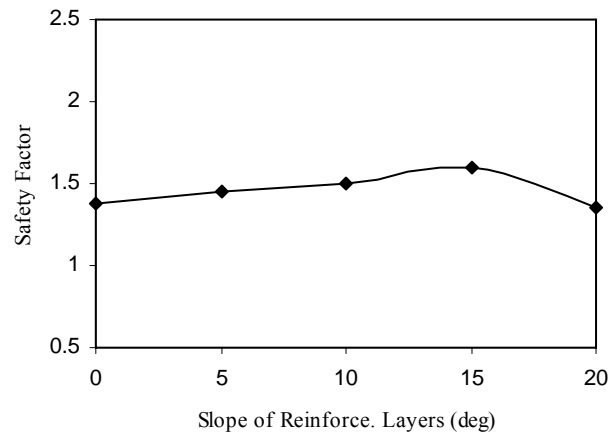


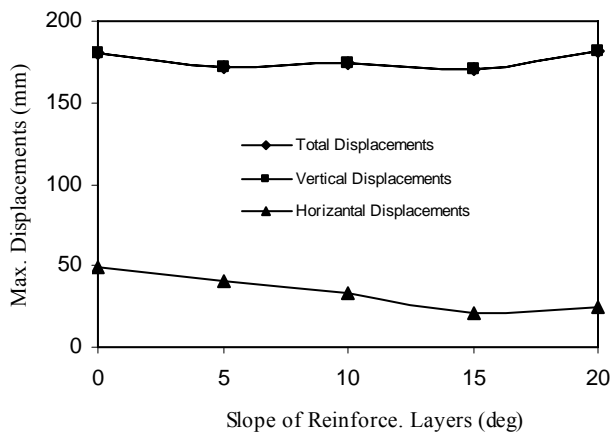
Figure 10. Computed effect of the reinforcement lengths on the same variables as in figure 5.



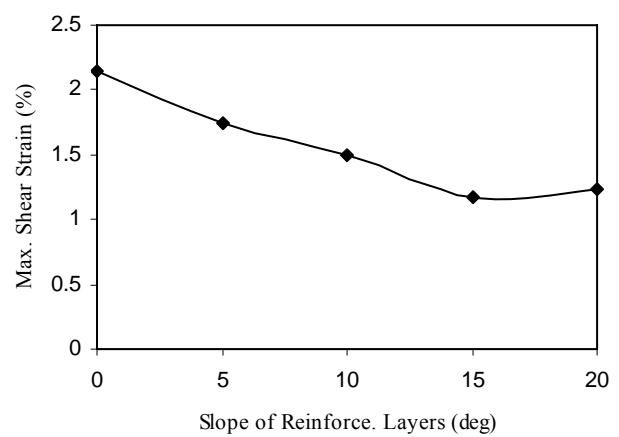
(a)



(b)



(c)



(d)

Figure 11. Computed effect of reinforcement slope angle on the same variables as in figure 5.

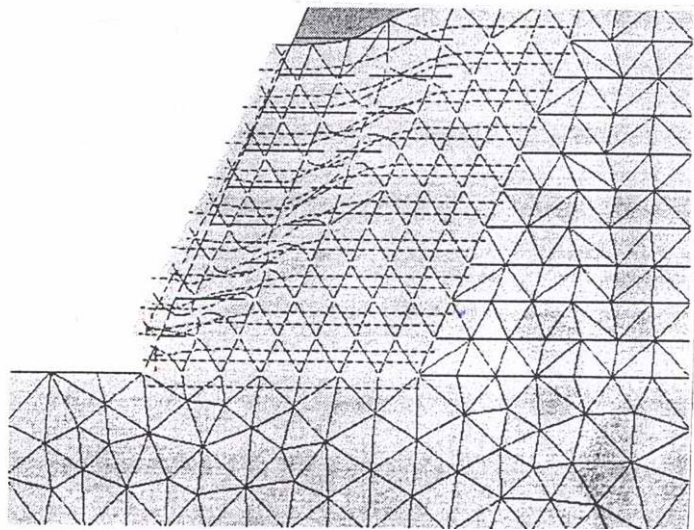


Figure 12. An example of the deformed mesh of the vertical cross section of a reinforced slope.

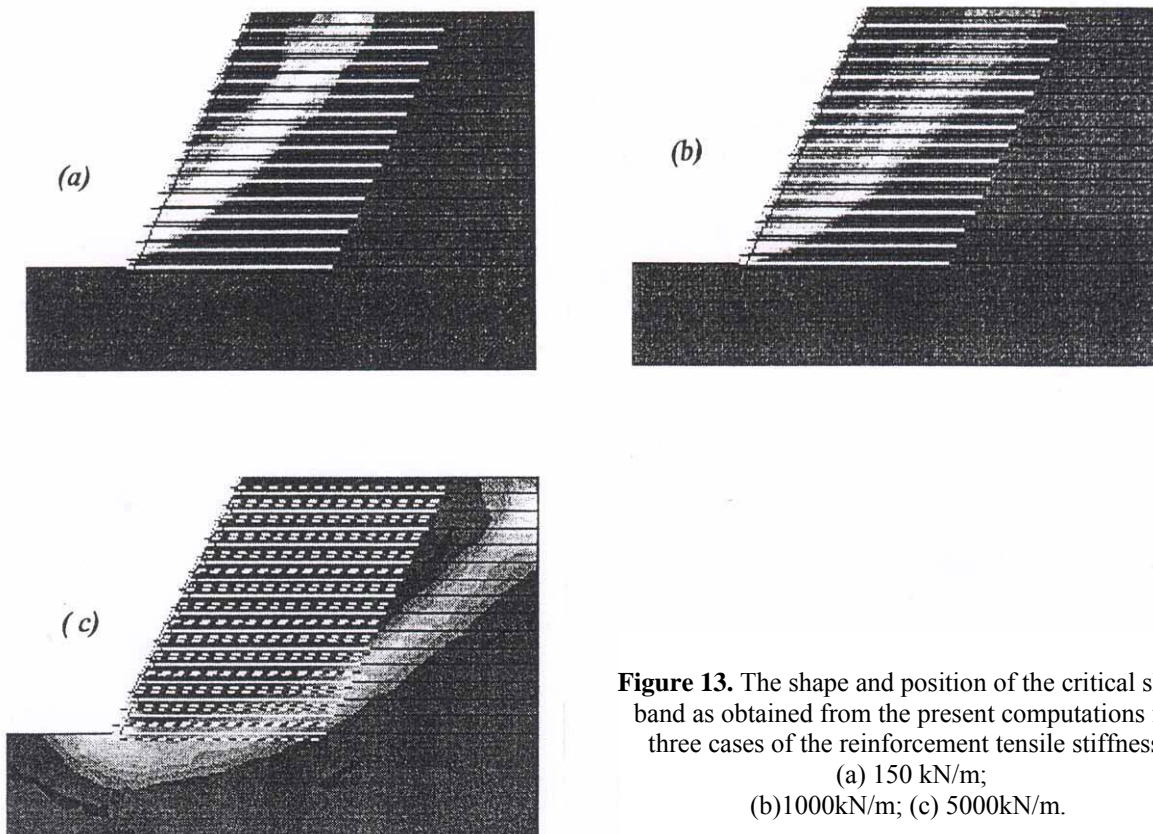


Figure 13. The shape and position of the critical shear band as obtained from the present computations for three cases of the reinforcement tensile stiffness:
 (a) 150 kN/m;
 (b) 1000 kN/m; (c) 5000 kN/m.

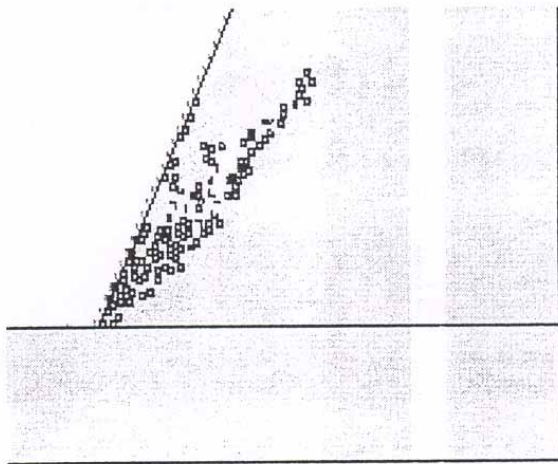


Figure 14. Location of plastic and tension points determined by PLAXIS

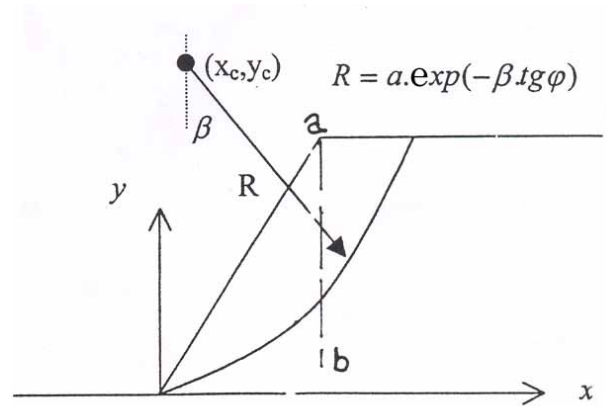


Figure 15. Geometrical feature for an assumed spiral or circle curve.

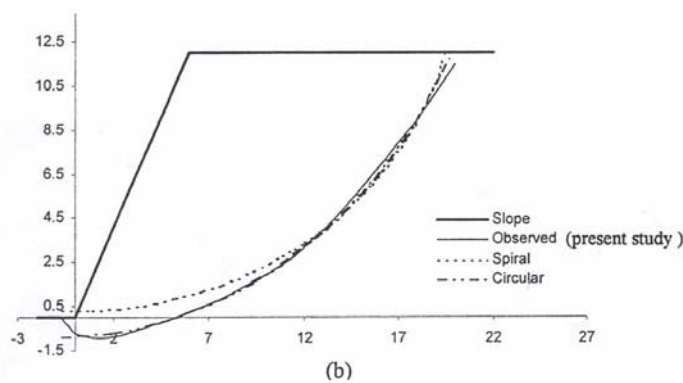
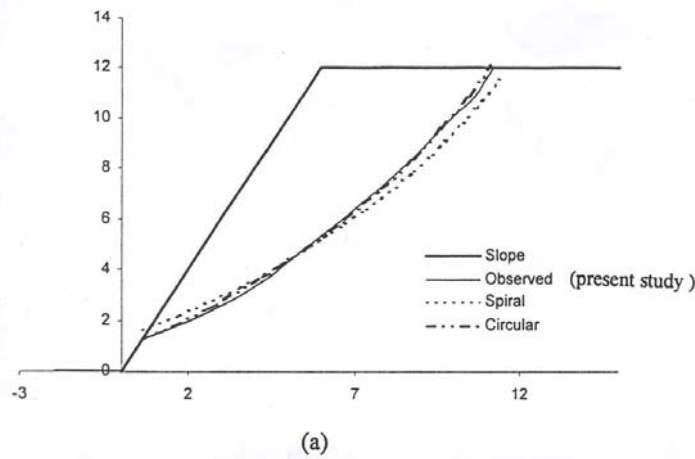
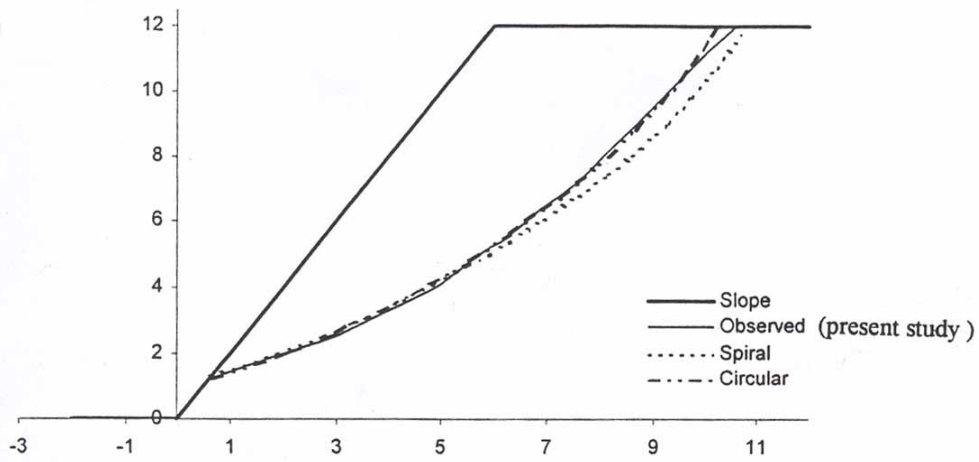
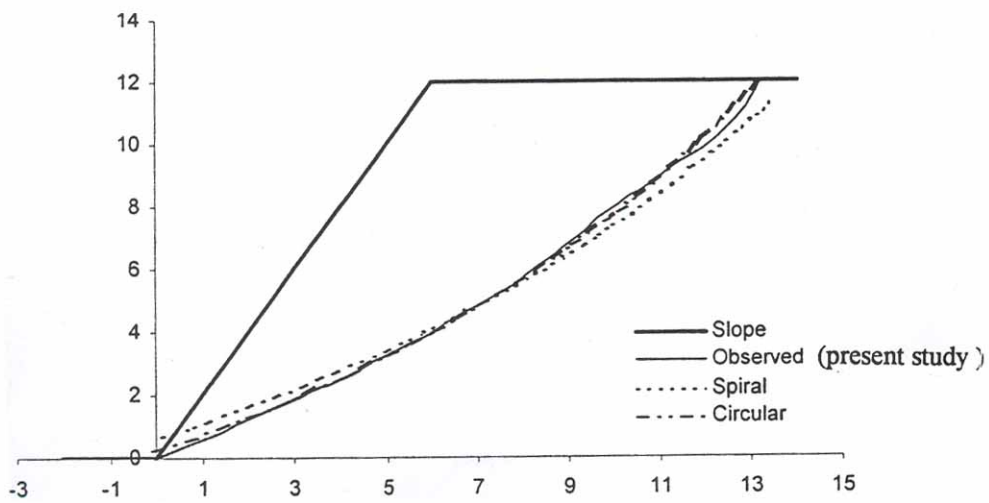


Figure 16. Comparison between the failure shape achieved by the present analysis (PLAXIS) and the best fitted curves of circle and spiral for two values of EA: (a) 150; and (b) 5000kN/m.



(a)



(b)

Figure 17. Comparison between the failure shape achieved by the present analysis (PLAXIS) and the best fitted curves of circle and spiral for two different amounts of number of reinforced layers: (a) 10 ; and (b) 30.

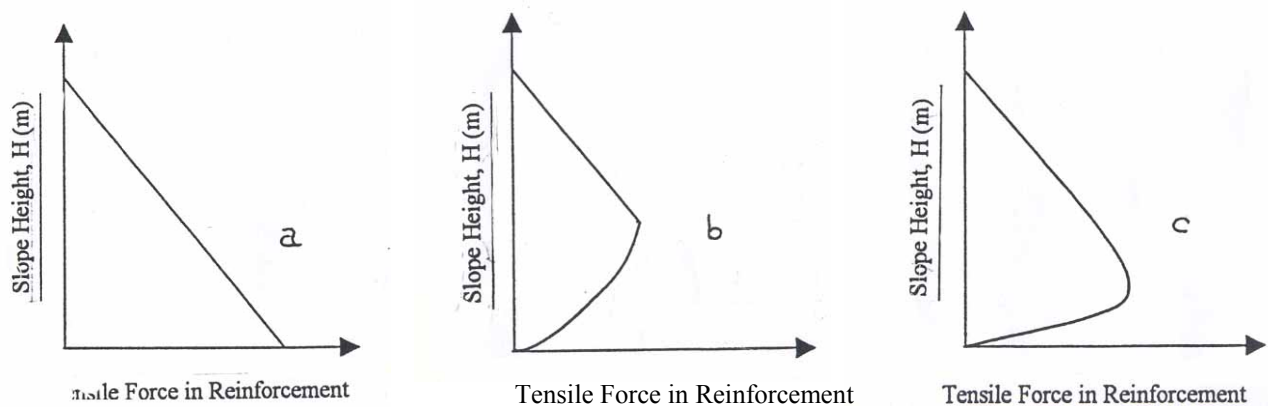


Figure 18. Comparison between different shapes of distribution of tensile forces in the reinforced layers along the height: (a) experimental; (b) analytical; and (c) present study.

5. CONCLUSIONS

From the results obtained in this study, the following can be concluded:

- 1) The shape of relative distribution of tensile force along the wall height is rather independent of the length of reinforcement layers, their tensile stiffness, their number, and their slope angle to the horizontal axis, and also independent of the height of slope and soil properties such as friction angle and dilatancy angle. The distribution of tensile force within reinforcements is shown in Figure 18a.
- 2) The position of the reinforcement layer on which maximum tensile force occurs is located at an elevation of 13 to 17 percent of the total height, and this position is rather independent of the above-mentioned variables. However, the location of maximum tensile force on the reinforcement is solely dependent on the slope angle of the wall, and this location moves upward with reduced slope angle.
- 3) Increasing tensile stiffness and length of reinforcement elements can result in increased safety factor of the slope and decreased

deformations and shear strains; however, these effects are limited to up to certain values after which they fail to show any significant effects.

- 4) Because the computed strains at the failure are not small, it is concluded that the mobilized friction angle of soil at the failure is the residual friction angle. Also, the dilatancy angle seems to have no obvious effects on the behavior of reinforced soil.
- 5) Within the reinforced slopes with reinforcing elements of axial stiffness below 1000 kN/m, the point of maximum shear strain on the failure surface is nearly located at the intersection of the vertical line through the edge of the slope and the slip surface.
- 6) The cross section of failure surface is fitted with a circular arc, though it is even possible to coincide with a curve of logarithmic spiral with lower accuracy.
- 7) The location of critical surface (shear band) in the cases studied depends, obviously, upon the overall stiffness of reinforced layers, so that by increasing the stiffness, the location of this surface moves farther from the slope face.

6. ACKNOWLEDGEMENT

The numerical and graphical results reported in this paper are due to R. Qaderi in his unpublished dissertation submitted to the Civil Engineering Department, Isfahan University of Technology, Iran, for the Degree of Masters in Civil

Engineering (1999?). The authors would like to express their gratitude to IUT for their permission to publish the results from the dissertation. We would also like to thank Mr. Ezzatollah Roustazadeh from the English Language Center, IUT, for her time editing the first draft of this paper.

Table 2. Properties and model characteristics for finding the best fitting curve

Model and Properties		Logarithmic spiral				Circular			
		x	Y	A	MSE	X	Y	R	MSE
EA KN/m	150	4.32	20.75	17	0.311	-9.21	19.66	20.92	0.08
	1000	6.54	24.01	19.95	.426	-12.84	26.42	29.48	0.08
	2000	7.22	28.47	23.95	.419	-12.27	27.25	29.95	0.05
	3000	13.83	29.81	23.05	.48	-7.98	32.78	33.93	0.07
	5000	13.94	19.56	15	.535	-.93	22.30	23.15	0.16
N=	10	4.62	26.87	22.8	.38	-12.39	24.2	26.42	0.07
	15	2.72	32.58	30.37	.46	-13.98	24.6	27.8	0.09
	30	6.63	33.42	28.88	.38	-13.47	28.72	31.48	0.1
1H:	1V	10.22	29.17	23.44	.36	-9.23	28.47	29.94	0.05
	2V	3.86	28.95	26.04	.4	-13.59	24.02	27.64	0.07
	3V	1.23	37.2	35.88	.49	-13.65	22.92	26.05	0.12
H(m)	6	1.88	17.06	15.12	.21	-8.04	14.48	16.28	0.05
	12	4.44	26.87	22.8	.38	-12.39	24.21	26.43	0.07
	18	7.52	37.45	31.55	.504	-19.68	37.87	41.88	0.17
$\Phi(^{\circ})$	30	9.14	23.1	18.87	.38	-6.33	23.06	23.57	0.07
	37	3.74	28.95	26.04	.4	-13.59	24.02	27.44	0.07
	45	2.43	28.49	26.67	.45	-13.29	21.28	25.18	0.27

6. REFERENCES

1. **Chalaturnyk R. J., Scott J. D., Chan D. H. K. and Rechards E.A.** Stresses and deformations in reinforced soil slopes; Canadian Geotechnical Journal, Vol. 27, pp. 232- 244, 1990
2. **Fannin R. J. and Hermann S.,** Performance data for a sloped reinforced soil wall; Canadian Geotechnical Journal, Vol. 27, pp. 676 – 686, 1990
3. **Ghinelli A. and Sacchetti M.,** Finite element analysis of instrumented geogrid reinforced slope; Proc. of Int. Conf. on Geosynthetics, Vol. 2, pp. 649- 654, 1998
4. **Han J., Leshchinsky D. and Shao Y.,** Influence of tensile stiffness of geosynthetic reinforcements on performance of reinforced slopes. Proc. 7th International Conf. on Geosynthetics, France, Delmas and Gourc (edit.), Vol. 1, 2002, pp. 197- 200
5. **Ingold T. S.,** Reinforced Earth, 1982
6. **Jewell R. A.,** Soil Reinforcement with geotextiles CIRIA, Special Publication 123, 1996
7. **Jewell R.A.,** Revised design charts for steep reinforced slopes, Reinforced Embankment, theory and Practice, pp. 1-30 Thomas Telford, London, 1991
8. **Leshchinsky D.,** Design dilemma: Use peak or residual strength of soil; Geotextiles and Geomembranes, Vol. 19, 2001, pp.111-125
9. **Leshchinsky D. and Boedeker R.H.,** Geosynthetic reinforced soil structures, ASCE, J of Geotech. Eng., Vol. 115, No. 10, 1989, pp. 1459- 1478
10. **Leshchinsky D.,** Stability of Geosynthetic reinforced steep slopes, Slope Stability Engineering, 1999, pp. 49-66
11. **Michalewich Z.,** Generic algorithm + data structure = evolution programs , Springer – Verlag, Berlin, Heidelberg, 1992
12. **Michalowski R.L.,** Stability of uniformly reinforced slopes; ASCE, J. of Geotec. and Geoenv. Eng. Vol. 123, No. 6, 1990, pp. 546- 556.
13. **Plaxis Manual,** Version 7.2 A.A. Balkema, Netherlands, 1998
14. **Porbaha A. and Kobayashi M.,** An Investigation of Hazard in Reinforced Embankment, *Geotechnical Hazards*, 1998, pp. 251-258
15. **Qhaderii R.** Study of stability of geosynthetically reinforced slope by application of finite element program of Plaxis 2D., M.Sc. Thesis, Soil Mechanics and Found. Eng. Group, Civil Engineering Department of IUT, Iran, 2003
16. **Reugger R.,** Geotextile reinforced soil structure, Proc. Third Int. Conf. on Geotextile, Vienna, Austria, 1986, pp. 453-654
17. **Sawicki A. and Lesniewska D.,** Limit Analysis of Cohesive Slopes Reinforced with Geotextiles, *Computers and Geotechnics*, Vol. 7, No. 1, 1989, pp. 53-66
18. **Schmertmann G. R., Chourey-Curties V. E., Johnson R. D. and Bonapart R.** Design Charts for geogrid-reinforced soil slopes *Proc. Geosynthetics, Industrial Fabrics Assn., Int. St. Paul, Minn., Vol. 1, 1987, pp. 108-120*
19. **Vidal H. (1969a),** The principles of reinforced earth. Highway Res. Rec., No. 282, pp. 1-16
20. **Wright S. G. and Duncan J. M.,** Limit Equilibrium Stability Analysis for Reinforced slopes, *Transp. Res. 1330, Transp. Res. Board,* Washington, 1991, pp. 40-46
21. **Zornberg J.G., Sitar n. and Mitchel J.K.,** Limit equilibrium as basis for design of geosynthetic reinforced slopes, ASCE, J. of Geotech. & Geoenv. Eng., Vol. 124, No. 8, 1998, pp. 684- 698
22. **Zorenberg J. G. and Arriaga F.,** Reinforced Soil Design: Integration of digital image analysis, numerical modeling and limit equilibrium, Technical Report, Colorado Advanced Software Institute, 2000, USA